Proceedings of IMECE2002
ASME International Mechanical Engineering Congress & Exposition
November 17–22, 2002, New Orleans, Louisiana

IMECE2002-33420

INDIRECT NEURAL NETWORK ADAPTIVE ROBUST CONTROL OF LINEAR MOTOR DRIVE SYSTEM *

J. Q. Gong
School of Mechanical Engineering
Purdue University, West Lafayette, IN 47907
Email: gong2@ecn.purdue.edu

Bin Yao
School of Mechanical Engineering
Purdue University, West Lafayette, IN 47907
Email: byao@ecn.purdue.edu

ABSTRACT

In this paper, an indirect neural network adaptive robust control (INNARC) scheme is developed for the precision motion control of linear motor drive systems. The proposed INNARC achieves not only good output tracking performance but also excellent identifications of unknown nonlinear forces in system for secondary purposes such as prognostics and machine health monitoring. Such dual objectives are accomplished through the complete separation of unknown nonlinearity estimation via neural networks and the design of baseline adaptive robust control (ARC) law for output tracking performance. Specifically, recurrent neural network (NN) structure with NN weights tuned on-line is employed to approximate various unknown nonlinear forces of the system having unknown forms to adapt to various operating conditions. The design is actual system dynamics based, which makes the resulting on-line weight tuning law much more robust and accurate than those in the tracking error dynamics based direct NNARC designs in implementation. With a controlled learning process achieved through projection type weights adaptation laws, certain robust control terms are constructed to attenuate the effect of possibly large transient modelling error for a theoretically guaranteed robust output tracking performance in general. Experimental results are obtained to verify the effectiveness of the proposed INNARC strategy. For example, for a typical point-to-point movement, with a measurement resolution level of $\pm 1\mu m$, the output tracking error during the entire execution period is within $\pm 5\mu m$ and mainly stays within $\pm 2\mu m$ showing excellent output tracking performance. At the same time, the outputs of NNs approximate the unknown forces very well allowing the estimates to be used for secondary purposes such as prognostics.

*THE WORK IS SUPPORTED IN PART BY THE NATIONAL SCIENCE FOUNDATION UNDER THE CAREER GRANT CMS-9734345.

INTRODUCTION

By eliminating mechanical transmissions and the associated transmission problems such as the structural flexibility and backlash [1; 2; 3], direct drive linear motors show great promise for widespread use in high-accuracy positioning systems. However, this class of drive systems also lose the advantage of using mechanical transmissions – gear reduction reduces the effect of model uncertainties such as parameter variations (e.g., uncertain payloads) and external disturbance (e.g., cutting forces in machining). Thus, to achieve the goal of having high precision movements, various uncertain nonlinearities including frictions, which are directly transmitted to the load and have significant effect on motion, need to be explicitly considered in controller design.

Although many efforts have been put into the research of modeling of friction [4; 5; 6], it may not be easy to integrate them into the controller design, due to either the complexity of model or the inaccuracy of model. How to bypass this problem is one of main focuses of this paper. Due to their universal approximation capability [7; 8; 9; 10; 11], neural network (NN) is employed in this paper to approximate all the unknown nonlinearities in system. In this way, the complex model of friction does not appear in controller design so that the process of controller design can be simplified. Since the characteristics of linear motors may vary from one to the other, on-line estimation of friction is necessary, which requires the on-line tuning of NN weights. There are two main issues to be considered for this purpose. Firstly, certain algorithms have to be derived to tune the unknown NN weights. Secondly, since the modeling error could be large during the training period, the issue of ro-

bustness to the approximation error needs to be taken into account. Although NN based control designs have been extensively investigated in [12; 13; 14; 15; 16], the transient performance of the closed-loop system cannot be guaranteed and the tracking error during the transient period may be large, which makes the design unattractive to industry. To avoid this shortcoming, the direct neural network adaptive robust control (DNNARC) has been recently proposed in [17; 18; 19], which preserves advantages of both the direct adaptive robust control (ARC) [20; 21; 22] and learning capability of NNs.

Experimental results obtained in [18] has demonstrated the excellent output tracking performance of the proposed DNNARC. However, a closer examination of the outputs of individual NNs reveals that the outputs of NNs can only capture the features of nonlinear forces reasonable well and the quality of the approximations is quite sensitive to neglected factors such as noises. Such a practical limitation is inherited to the direct NN control designs, as the NN weight tuning laws and the underline ARC laws are synthesized jointly through a Lyapunov function with the sole goal of reducing output tracking errors. Such an approach restricts the choice of the tuning laws of NN weights to gradient type with certain actual tracking errors as driving signals. As the actual tracking errors are rather small in implementation, they are prone to be corrupted by neglected factors such as measurement noises, which makes the accurate estimations of individual unknown nonlinear forces rather difficult. To avoid these shortcoming of direct NN designs and further exploit the good theoretical approximation potential of NNs, an indirect neural network adaptive robust control (INNARC) is developed in this paper. The proposed approach totally separates the construction of suitable NNs for accurate unknown nonlinearity estimation from the design of underline ARC law for a guaranteed robust output tracking performance. As such, there is no more one-stone-two-birds problem, which makes the dual objectives of having both excellent output tracking performance and good nonlinearity estimation a realist goal in implementation. Experimental results have been obtained verifying the effectiveness of the proposed INNARC approach.

The rest of the paper is organized as follows: firstly, the model of linear motor drive system and control problem is presented; it is followed by the approximation property of neural network; then, based on the assumption that all the input-hidden weights are known, RNN identifier and INNARC are designed; subsequently, the case that all of the NN weights are unknown is discussed; after all of these theoretical preparations, experiments are carried out, followed by some conclusions drawn at last.

LINEAR MOTOR MODEL AND PROBLEM FORMULATION

The mathematical model of a linear motor drive system with negligible electrical dynamics can thus be described by [18]

$$M\ddot{y} = u - B\dot{y} - F_{fn}(y,\dot{y}) - F_r(y,\dot{y}) + F_d \qquad (1)$$

where y represents the position of the inertia load, M is the normalized[†] mass of the inertia load plus the coil assembly, u is the input voltage to the motor, B is the equivalent viscous friction coefficient of the system, F_{fn} is the normalized nonlinear Coloumb friction term, F_r represents the normalized electro-magnetic force ripple, and F_d represents the normalized external disturbance force (e.g. cutting force in machining). Eq. (1) can be written into the following state-space form

$$\begin{aligned}\dot{x}_1 &= x_2\\ \dot{x}_2 &= \underbrace{-\frac{B}{M}x_2 - \frac{1}{M}F_a(x_1,x_2)}_{f_2(x_1,x_2)} + \underbrace{\frac{1}{M}}_{b_2(x_1,x_2)}\ u - \underbrace{\frac{1}{M}F_d(x_1,x_2)}_{\Delta_2}\end{aligned} \qquad (2)$$

where $x_1 = y$ and $x_2 = \dot{y}$, and $F_a \triangleq F_{fn}(x,\dot{x}) + F_r(x,\dot{x})$. In (2), for generality, all state-dependent unkwnon nonlinearities are lumped together as a general unknown nonlinear function $f_2(x_1,x_2)$ and b is assumed to depend on states as well.

Although many models have been proposed for the nonlinear friction, it is still in general difficult to know the exact form of the friction. As such, in this paper, a three-layer feedforward neural network is constructed to approximate the nonlinearity f_2, which is detailed in the following assumption

Assumption 1. *The NN approximation error associated with the nonlinear function f_2 is assumed to be bounded by [8],*

$$|f_2(\bar{x}_2) - \boldsymbol{w}_{f_2}^T \boldsymbol{g}_{f_2}(\boldsymbol{V}_{f_2}\bar{x}_{a_2})| \le \delta_{f_2}(\bar{x}_2), \quad \forall \bar{x}_2 \in \mathcal{R}^2 \qquad (3)$$

where $\bar{x}_2 = [x_1, x_2]^T$ is the state vector, $\bar{x}_{a_2} = [\bar{x}_2^T, -1]^T$ is the augmented input vector to the neural network (-1 term denotes the input bias), $\boldsymbol{w}_{f_2} = [w_{f_2,1}, \cdots, w_{f_2,r_{f_2}}]^T$ is the optimal hidden-output weight vector, $\boldsymbol{V}_{f_2} = [\boldsymbol{v}_{f_2,1}, \cdots, \boldsymbol{v}_{f_2,r_{f_2}}]^T \in \mathcal{R}^{r_{f_2}\times 3}$ is the optimal input-hidden weight matrix with $\boldsymbol{v}_{f_2,j} \in \mathcal{R}^{3\times 1}$, r_{f_2} is the number of neurons in the hidden layer, and $\boldsymbol{g}_{f_2}(\boldsymbol{V}_{f_2}\bar{x}_{a_2}) = [g_{f_2,1}(\boldsymbol{v}_{f_2,1}^T\bar{x}_{a_2}), \cdots, g_{f_2,r_{f_2}}(\boldsymbol{v}_{f_2,r_{f_2}}^T\bar{x}_{a_2})]^T$ is the activation function vector, and $\delta_{f_2}(\bar{x}_2)$ is a non-negative known shape function.

[†]Normalized with respect to the unit input voltage.

Assumption 2. *Similarly, it is also assumed b_2 can be approximated by the output of a three-layer feedforward NN as follows*

$$|b_2 - \boldsymbol{w}_{b_2}^T \boldsymbol{g}_{b_2}(\boldsymbol{V}_{b_2}\bar{x}_{a_2})| \leq \delta_{b_2}(\bar{x}_2),\ \forall \bar{x}_2 \in \mathcal{R}^2, \qquad (4)$$

where $\boldsymbol{w}_{b_2}$, $\boldsymbol{g}_{b_2}$, $\boldsymbol{V}_{b_2}$, and δ_{b_2} are defined in similar ways as $\boldsymbol{w}_{f_2}$, $\boldsymbol{g}_{f_2}$, $\boldsymbol{V}_{f_2}$, and δ_{f_2} in **Assumption 1**, *respectively. It is assumed that the number of neurons in the hidden-layer is r_{b_2}. The dimensions of $\boldsymbol{w}_{b_2}$, $\boldsymbol{g}_{b_2}$, and $\boldsymbol{V}_{b_2}$ can be decided accordingly.*

Furthermore, without loss of generality, the following assumption is made

Assumption 3. *The input gain b_2 is nonzero with known sign, and $b_2 \geq b_{l,2} > 0$, $\forall \bar{x}_2 \in \mathcal{R}^2$, where $b_{l,2}$ is a known positive constant representing the lower bound of b_2.*

While it is usually difficult to predict the type of disturbances that the system is going to encounter, it is reasonable to assume that the disturbance is bounded in certain way. Hence, the following practical assumption is made

Assumption 4. *The time-varying nonlinearity Δ_2 is bounded by $|\Delta_2| \leq \delta_{\Delta_2}(\bar{x}_2, t)$, where $\delta_{\Delta_2}(\bar{x}_2, t)$ is a non-negative known function of $\bar{x}_2$ and time t.*

The control objective is to drive the system output $y = x_1$ to follow a smooth desired trajectory y_d as quickly and closely as possible in spite of unknown nonlinearities in system. At the same time, since f_2 and b_2 are unknown, certain mechanism is needed to approximate the dynamics described in the second equation of (2). In the following discussion, some shorthands of notations will be used: $\boldsymbol{g}_{f_2} = \boldsymbol{g}_{f_2}(\boldsymbol{V}_{f_2}\bar{x}_{a_2})$, $\boldsymbol{g}_{b_2} = \boldsymbol{g}_{b_2}(\boldsymbol{V}_{b_2}\bar{x}_{a_2})$, $\hat{\boldsymbol{g}}_{f_2} = \boldsymbol{g}_{f_2}(\hat{\boldsymbol{V}}_{f_2}\bar{x}_{a_2})$, $\hat{\boldsymbol{g}}_{b_2} = \boldsymbol{g}_{b_2}(\hat{\boldsymbol{V}}_{b_2}\bar{x}_{a_2})$, $f_2^* = \boldsymbol{w}_{f_2}^T \boldsymbol{g}_{f_2}$, and $b_2^* = \boldsymbol{w}_{b_2}^T \boldsymbol{g}_{b_2}$. Without introducing ambiguity, $\hat{f}_2 = \hat{\boldsymbol{w}}_{f_2}^T \hat{\boldsymbol{g}}_{f_2}$, when $\hat{\boldsymbol{V}}_{f_2}$ is used; or $\hat{f}_2 = \hat{\boldsymbol{w}}_{f_2}^T \boldsymbol{g}_{f_2}$, when $\boldsymbol{V}_{f_2}$ is known. $\hat{g}_2$ is defined in the same way.

APPROXIMATION PROPERTY OF NEURAL NETWORKS

Lemma 1. *For a neural network with $\boldsymbol{x}_{\{in\}} \in \mathcal{R}^{p+1}$ being its input vector, $\boldsymbol{V} = [\boldsymbol{v}_1, \cdots, \boldsymbol{v}_{r_n}]^T \in \mathcal{R}^{r_n \times (p+1)}$ being its input-hidden weight matrix, $\boldsymbol{g}$ being the activation function vector, $\boldsymbol{w} \in \mathcal{R}^{m \times r_n}$ being its hidden-output weight matrix, The output of neural network $\boldsymbol{w}^T \boldsymbol{g}(\boldsymbol{V}\boldsymbol{x}_{\{in\}})$ can be approximated by its estimate $\hat{\boldsymbol{w}}^T \boldsymbol{g}(\hat{\boldsymbol{V}}\boldsymbol{x}_{\{in\}})$ by the following form*

$$\boldsymbol{w}^T\boldsymbol{g} = \hat{\boldsymbol{w}}^T\hat{\boldsymbol{g}} - \tilde{\boldsymbol{w}}^T(\hat{\boldsymbol{g}} - \hat{\boldsymbol{g}}'\hat{\boldsymbol{V}}\boldsymbol{x}_{\{in\}}) - \hat{\boldsymbol{w}}^T\hat{\boldsymbol{g}}'\tilde{\boldsymbol{V}}\boldsymbol{x}_{\{in\}} + d_{NN} \quad (5)$$

where $\hat{\boldsymbol{g}} = \boldsymbol{g}(\hat{\boldsymbol{V}}\boldsymbol{x}_{\{in\}})$, $\hat{\boldsymbol{g}}' = diag\{\hat{g}_1', \cdots, \hat{g}_r'\}$ with $\hat{g}_i' = g_i'(\hat{\boldsymbol{v}}_i^T\boldsymbol{x}_{\{in\}}) = \frac{dg_i(z)}{dz}|_{z=\hat{\boldsymbol{v}}_i^T\boldsymbol{x}_{\{in\}}}$, $i = 1, \cdots, r_n$, and residual term $d_{NN} = -\tilde{\boldsymbol{w}}^T\hat{\boldsymbol{g}}'\boldsymbol{V}\boldsymbol{x}_{\{in\}} + \boldsymbol{w}\mathcal{O}(\tilde{\boldsymbol{V}}\boldsymbol{x}_{\{in\}})$ with $\mathcal{O}(\tilde{\boldsymbol{V}}\boldsymbol{x}_{\{in\}})$ being the sum of the higher order terms. The residual term d_{NN} can be bounded by a linear-in-parameter function as $||d_{NN}||_2 \leq \boldsymbol{\beta}^T\boldsymbol{Y}$ [23], where $\boldsymbol{\beta}$ is an unknown vector constituting of positive elements, and the known function vector $\boldsymbol{Y}$ is defined as $\boldsymbol{Y} = \left[1, ||\boldsymbol{x}_{\{in\}}||_2, ||\hat{\boldsymbol{w}}||_F||\boldsymbol{x}_{\{in\}}||_2, ||\hat{\boldsymbol{V}}||_F||\boldsymbol{x}_{\{in\}}||_2\right]^T$ with $||\bullet||_2$ being the 2-norm of a vector $\bullet$, and $||\bullet||_F$ denoting the Frobenius norm of a matrix $\bullet$, which is defined as $||\bullet||_F^2 = \text{Trace}\{\bullet^T\bullet\}$. ◇

By applying the above lemma to continuous nonlinear functions f_2 and b_2, we have

$$f_2^* = \hat{f}_2 - \tilde{\boldsymbol{w}}_{f_2}^T(\hat{\boldsymbol{g}}_{f_2} - \hat{\boldsymbol{g}}_{f_2}'\hat{\boldsymbol{V}}_{f_2}\bar{x}_{a_2}) - \hat{\boldsymbol{w}}_{f_2}^T\hat{\boldsymbol{g}}_{f_2}'\tilde{\boldsymbol{V}}_{f_2}\bar{x}_{a_2} + d_{f_2,NN} \quad (6)$$

$$b_2^* = \hat{b}_2 - \tilde{\boldsymbol{w}}_{b_2}^T(\hat{\boldsymbol{g}}_{b_2} - \hat{\boldsymbol{g}}_{b_2}'\hat{\boldsymbol{V}}_{b_2}\bar{x}_{a_2}) - \hat{\boldsymbol{w}}_{b_2}^T\hat{\boldsymbol{g}}_{b_2}'\tilde{\boldsymbol{V}}_{b_2}\bar{x}_{a_2} + d_{b_2,NN} \quad (7)$$

$$|d_{f_2,NN}| \leq \boldsymbol{\beta}_{f_2}^T\boldsymbol{Y}_{f_2},\ |d_{b_2,NN}| \leq \boldsymbol{\beta}_{b_2}^T\boldsymbol{Y}_{b_2} \quad (8)$$

where all the notations are defined in the same way as in the above lemma.

INNARC DESIGN WITH KNOWN INPUT-HIDDEN LAYER WEIGHTS

In this section, based on the assumption that all the input-hidden weights in both neural networks are known, RNN will be used in the construction of the identifier, and then INNARC will be developed accordingly.

Design and Stability Analysis of RNN Identifier

Since the first dynamic equation in (2) is exactly known, only the second equation needs to be approximated. Based on its structure, the following RNN identifier is proposed

$$\dot{\hat{x}}_2 = -a_2 e_2 + \hat{f}_2 + \hat{b}_2 u + u_{iden,2} \quad (9)$$

where $\hat{x}_2$ is the estimate of x_2, $a_2 = a_{2,1} + a_{2,2}$ with both $a_{2,1}$ and $a_{2,2}$ being positive constants, $e_2 = \hat{x}_2 - x_2$ is the identification error, and $u_{iden,2}$ is a smooth function of e_2 satisfying the following condition [19]

$$\begin{matrix} e_2 u_{iden,2} \\ e_2\left[(\hat{f}_2 - f_2) + (\hat{b}_2 - b_2)u - \Delta_2 + u_{iden,2}\right] \end{matrix} \begin{matrix} \leq 0 \\ \leq \epsilon_{e2} \end{matrix} \quad (10)$$

with

$$\epsilon_{e2} = \left|1 + \frac{|(||\rho_{wf_2}||_2 - ||\hat{\rho}_{wf_2}||_2)|}{||\hat{\rho}_{wf_2}||_2}\right|^2 \epsilon_{e2,1} + \left|1 + \frac{|(||\rho_{wb_2}||_2 - ||\hat{\rho}_{wb_2}||_2)|}{||\hat{\rho}_{wb_2}||_2}\right|^2 \epsilon_{e2,2}, \quad (11)$$

ρ_{wf_2} and ρ_{wb_2} are bounds of $\boldsymbol{w}_{f_2}$ and $\boldsymbol{w}_{b_2}$ respectivley, and $\hat{\rho}_{wf_2}$ and $\hat{\rho}_{wb_2}$ are fictitious ones [19]. $u_{iden,2}$ can be chosen in the same way as in [19].

Remark 1. *Based on the fact that $u_{iden,2}$ is a smooth function of e_2 and $e_2 u_{iden_2} \leq 0$, it can be proven that $\lim_{e_2 \to 0} u_{iden,2} = 0$.*

Proof. *Since it is a smooth function of e_2, $u_{iden,2}$ is a continuous function of e_2, and $\lim_{e_2 \to 0} u_{iden,2}(e_2) = u_{iden,2}(0)$. It only needs to prove that $u_{iden,2}(0) = 0$.*

Suppose that $u_{iden,2}(0) > 0$, then there is a neighborhood $[-n_l, n_r]$ of 0 with $n_l > 0$, and $n_r > 0$, such that $u_{iden,2}(n_m) > 0$, $\forall n_m \in [-n_l, n_r]$ due to the smoothness of $u_{iden,2}$. Choose $n_m = \frac{n_r}{2}$, which is greater than 0. Then we have $n_m u_{iden,2}(n_m) > 0$, which contradicts the condition $e_2 u_{iden,2} \leq 0$, $\forall e_2$. Similarly, it can also be shown that $u_{iden,2}(0) < 0$ does not hold. Hence, $u_{iden,2}(0) = 0$. In conclusion, $lim_{e_2 \to 0} u_{iden,2}(e_2) = u_{iden,2}(0) = 0$. □

Subtracting the second equation (2) from (9) results in the following identification error dynamic

$$\dot{e}_2 = -a_2 e_2 + [f_2^* - f_2] + \left[\hat{f}_2 - f_2^*\right] + [b_2^* - b_2]\, u + \left[\hat{b}_2 - b_2^*\right] u + u_{iden,2} - \Delta_2 \quad (12)$$

The above identification error dynamic equation can also be written in the following form

$$\dot{e}_2 = -a_2 e_2 + [f_2^* - f_2] + \tilde{\boldsymbol{w}}_{f_2}^T \boldsymbol{g}_{f_2} + [b_2^* - b_2]\, u + \tilde{\boldsymbol{w}}_{b_2}^T \boldsymbol{g}_{b_2} u + u_{iden,i} - \Delta_2 \quad (13)$$

Based on identification error equation(13), the following gradient type of tuning laws are proposed along with projection mapping [19]

$$\dot{\hat{\boldsymbol{w}}}_{f_2} = \mathbf{Proj}_{\hat{\boldsymbol{w}}_{f_2}}\left[\Gamma_{w,f_2} \tau_{I,\hat{\boldsymbol{w}}_{f_2}}\right], \quad \tau_{I,\hat{\boldsymbol{w}}_{f_2}} = -e_2 \boldsymbol{g}_{f_2}$$
$$\dot{\hat{\boldsymbol{w}}}_{b_2} = \mathbf{Proj}_{\hat{\boldsymbol{w}}_{b_2}}\left[\Gamma_{w,b_2} \tau_{I,\hat{\boldsymbol{w}}_{b_2}}\right], \quad \tau_{I,\hat{\boldsymbol{w}}_{b_2}} = -e_2 u \boldsymbol{g}_{b_2} \quad (14)$$

where Γ's are diagonal positive definite matrices, and τ's are tuning functions.

Remark 2. *It should be noted that other types of tuning laws can also be used to tune NN weights. In this paper, for the purpose of illustration, only gradient type of tuning laws are considered.* ◊

Theorem 1. *Using the identifier (9) along with tuning laws given in (14), the following results hold*

A. In general, estimates of NN weights are bounded, and the square of identification error e_2 exponentially converges to a region bounded in the following manner

$$lim_{t \to \infty} e_2^2(t) \leq \frac{1}{a_2} \epsilon_{e,2} \quad (15)$$

B. If there is no time-varying nonlinearity and the optimal NNs can match all the nonlinearities exactly, i.e., $\Delta_2 = \delta_{f_2} = \delta_{b_2} = 0$, and all the states x_i's and input u are bounded, then all identification error e_2 goes to zero asymptotically provided that true values of NN weights are within fictitious bounds.

C. If all the condition in Result **B** *holds and the following PE condition*

$$\exists T, T_0,\ s.t.,\ \int_t^{t+T} \underbrace{\begin{bmatrix} \boldsymbol{g}_{f_2} \boldsymbol{g}_{f_2}^T & \boldsymbol{g}_{f_2} \boldsymbol{g}_{b_2}^T u \\ u \boldsymbol{g}_{b_2} \boldsymbol{g}_{f_2}^T & u \boldsymbol{g}_{b_2} \boldsymbol{g}_{b_2}^T u \end{bmatrix}}_{\boldsymbol{M}_{pe}(\xi)} d\xi \geq \nu_l \boldsymbol{I}_{2n} > 0, \quad \forall t \geq T_0, \quad (16)$$

is also satisfied, all the estimates of hidden-output weights will also converge to the corresponding optimal values. ◊

Proof. **A.** By the property of projection mapping, the boundednesses of all the estimates of NN weights are guaranteed [19].

Consider Lyapunov function $V_e = \frac{1}{2} e_2^2$. Using the second condition in (10), it is known that

$$\dot{V}_e = e_2 \dot{e}_2 \leq -2 a_2 V_e + \epsilon_{e,2} \quad (17)$$

By comparison lemma, it can be shown that

$$V_e(t) \leq V_e(0) exp(-2a_2 t) + \epsilon_{e,2} \int_0^t exp(-2a_2(t-\tau)) d\tau \leq V_e(0) exp(-2a_2 t) + \frac{1}{2a_2} \epsilon_{e,2}, \quad (18)$$

which indicates that $V_e(t)$ exponentially decays to a region, and $lim_{t \to \infty} V_e(t) \leq \frac{1}{2a_2} \epsilon_{e,2}$. Hence, inequality (15) holds.

B. Consider the following Lyapunov function

$$V_{ea} = V_e + \left[\tilde{\boldsymbol{w}}_{f_2}^T \Gamma_{w,f_2}^{-1} \tilde{\boldsymbol{w}}_{f_2} + \tilde{\boldsymbol{w}}_{b_2}^T \Gamma_{w,b_2}^{-1} \tilde{\boldsymbol{w}}_{b_2}\right] \tag{19}$$

Following the assumptions $\delta_{f_2} = \delta_{b_2} = 0$, $f_2 = f_2^*$ and $b_2 = b_2^*$ hold. Furthermore, since $\Delta_2 = 0$, the identification error dynamic equation (13) is simplified into

$$\dot{e}_2 = -a_2 e_2 + \tilde{\boldsymbol{w}}_{f_2}^T \boldsymbol{g}_{f_2} + \tilde{\boldsymbol{w}}_{b_2}^T \boldsymbol{g}_{b_2} u + u_{iden,2} \tag{20}$$

Differentiating (19) results in

$$\begin{aligned} \dot{V}_{ea} &= \left\{-a_2 e_2^2 - e_2 \tilde{\boldsymbol{w}}_{f_2}^T \tau_{I,\hat{w}_{f_2}} - e_2 \tilde{\boldsymbol{w}}_{b_2}^T \tau_{I,\hat{w}_{b_2}} u + u_{iden,2} e_2\right\} \\ &\quad + \left\{\tilde{\boldsymbol{w}}_{f_2}^T \Gamma_{w,f_2}^{-1} \dot{\tilde{\boldsymbol{w}}}_{f_2} + \tilde{\boldsymbol{w}}_{b_2}^T \Gamma_{w,b_2}^{-1} \dot{\tilde{\boldsymbol{w}}}_{b_2}\right\} \\ &\leq -a_2 e_2^2 \end{aligned} \tag{21}$$

where the property of projection mapping is used [19]. It is then clear that V_{ea} is a positive semi-definite function. By Barbalat's lemma, it is obtained that $lim_{t\to} e_2 = 0$.

C. From the result in A, all the estimates are always bounded. Furthermore, from equation (20), it is also found that $\dot{e}_2$'s are bounded.

Differentiating both sides of (20) results in

$$\begin{aligned} \ddot{e}_2 &= -a_2 \dot{e}_2 + \dot{\tilde{\boldsymbol{w}}}_{f_2}^T \boldsymbol{g}_{f_2} + \tilde{\boldsymbol{w}}_{f_2}^T \dot{\boldsymbol{g}}_{f_2} + \dot{\tilde{\boldsymbol{w}}}_{b_2}^T \boldsymbol{g}_{b_2} u \\ &\quad + \tilde{\boldsymbol{w}}_{b_2}^T \dot{\boldsymbol{g}}_{b_2} u + \tilde{\boldsymbol{w}}_{b_2}^T \boldsymbol{g}_{b_2} \dot{u} + \frac{\partial u_{iden,2}}{\partial e_2} \dot{e}_2 \end{aligned} \tag{22}$$

From (22), it is clear that $\ddot{e}_2$ is bounded. Hence, $\dot{e}_2$ is a uniform continuous function of time. It is also true that $\int_0^\infty \dot{e}_2 dt = e_2(\infty) - e_2(0) = -e_2(0)$ since Result **B** shows that $e_2(\infty) = 0$. Then $\int_0^\infty \dot{e}_2 dt$ is bounded. By Barbalat's lemma, $lim_{t\to\infty} \dot{e}_2 = 0$ can be obtained.

From equation (20), it is known that $lim_{t\to\infty} \tilde{\boldsymbol{w}}_{f_2}^T \boldsymbol{g}_{f_2} + \tilde{\boldsymbol{w}}_{b_2}^T \boldsymbol{g}_{b_2} u = 0$. It follows that

$$\begin{aligned} &\lim_{t\to\infty} \left(\tilde{\boldsymbol{w}}_{f_2}^T \boldsymbol{g}_{f_2} + \tilde{\boldsymbol{w}}_{b_2}^T \boldsymbol{g}_{b_2} u\right)^2 = 0 \\ \Longleftrightarrow &\lim_{t\to\infty} \left[\tilde{\boldsymbol{w}}_{f_2}^T \; \tilde{\boldsymbol{w}}_{b_2}^T\right] \begin{bmatrix} \boldsymbol{g}_{f_2} \\ \boldsymbol{g}_{b_2} u \end{bmatrix} \left[\boldsymbol{g}_{f_2}^T \; \boldsymbol{g}_{b_2}^T u\right] \begin{bmatrix} \tilde{\boldsymbol{w}}_{f_2} \\ \tilde{\boldsymbol{w}}_{b_2} \end{bmatrix} = 0 \\ \Longleftrightarrow &\lim_{t\to\infty} \left[\tilde{\boldsymbol{w}}_{f_2}^T \; \tilde{\boldsymbol{w}}_{b_2}^T\right] \boldsymbol{M}_{pe} \begin{bmatrix} \tilde{\boldsymbol{w}}_{f_2} \\ \tilde{\boldsymbol{w}}_{b_2} \end{bmatrix} = 0 \end{aligned} \tag{23}$$

Since it has already been obtained that $\lim_{t\to\infty} e_2 = 0$, we have $\lim_{t\to\infty} \dot{\tilde{\boldsymbol{w}}}_{f_2} = 0$ and $\lim_{t\to\infty} \dot{\tilde{\boldsymbol{w}}}_{b_2} = 0$ from equations given in (14).

From (23), for any finite time interval T, it is obtained that

$$\lim_{t\to\infty} \int_t^{t+T} \left[\tilde{\boldsymbol{w}}_{f_2}^T(\xi) \; \tilde{\boldsymbol{w}}_{b_2}^T(\xi)\right] \boldsymbol{M}_{pe}(\xi) \begin{bmatrix} \tilde{\boldsymbol{w}}_{f_2}(\xi) \\ \tilde{\boldsymbol{w}}_{b_2}(\xi) \end{bmatrix} d\xi = 0 \tag{24}$$

Utilizing mean value theorem and noting the fact hat $\lim_{t\to\infty} \dot{\tilde{\boldsymbol{w}}}_{f_2} = 0$ and $\lim_{t\to\infty} \dot{\tilde{\boldsymbol{w}}}_{b_2} = 0$, equation (24) induces that

$$\begin{aligned} &\lim_{t\to\infty} \int_t^{t+T} \left[\tilde{\boldsymbol{w}}_{f_2}^T(t) \; \tilde{\boldsymbol{w}}_{b_2}^T(t)\right] \boldsymbol{M}_{pe}(\xi) \begin{bmatrix} \tilde{\boldsymbol{w}}_{f_2}(t) \\ \tilde{\boldsymbol{w}}_{b_2}(t) \end{bmatrix} d\xi = 0 \\ \Longleftrightarrow \\ &\lim_{t\to\infty} \left[\tilde{\boldsymbol{w}}_{f_2}^T(t) \; \tilde{\boldsymbol{w}}_{b_2}^T(t)\right] \int_t^{t+T} \boldsymbol{M}_{pe}(\xi) d\xi \begin{bmatrix} \tilde{\boldsymbol{w}}_{f_2}(t) \\ \tilde{\boldsymbol{w}}_{b_2}(t) \end{bmatrix} = 0 \end{aligned} \tag{25}$$

From condition (16), we arrive at

$$\left[\tilde{\boldsymbol{w}}_{f_2}^T \; \tilde{\boldsymbol{w}}_{b_2}^T\right] \int_t^{t+T} \boldsymbol{M}_{pe} d\xi \begin{bmatrix} \tilde{\boldsymbol{w}}_{f_2} \\ \tilde{\boldsymbol{w}}_{b_2} \end{bmatrix} \geq \nu_l \left\| \begin{bmatrix} \tilde{\boldsymbol{w}}_{f_2} \\ \tilde{\boldsymbol{w}}_{b_2} \end{bmatrix} \right\|^2 > 0, \tag{26}$$

$\forall t \geq T_0$. From equation (25) and inequality (26), it is obtained that $\lim_{t\to\infty} \left\| \begin{bmatrix} \tilde{\boldsymbol{w}}_{f_2} \\ \tilde{\boldsymbol{w}}_{b_2} \end{bmatrix} \right\|^2 = 0$, which is equivalent to $\lim_{t\to\infty} \tilde{\boldsymbol{w}}_{f_2} = 0$, and $\lim_{t\to\infty} \tilde{\boldsymbol{w}}_{b_2} = 0$. In conclusion, all the estimates of hidden-output weights converge to their optimal values asymptotically. □

Remark 3. *A of Theorem 1 shows that the error between of the RNN identifier and the true system can be made as small as possible. B of Theorem 1 shows that the identification error can possibly converge to zero. Hence, from the viewpoint of input-state relationship, RNN identifier (9) can be looked on as a good model of the true plant.* ♢

Remark 4. *By fast feedback, A of Theorem 1 shows that identification errors e_i's are always under the control of designer even when NNs do not match the unknown nonlinearities. With the help of tuning laws, B shows the possibility of asymptotic identification. Furthermore, if PE condition is satisfied, in addition to Results A and B, estimates of NN weights converge to their optimal value asymptotically, which fulfills the learning capability of NNs. Unlike what have been done in [24; 25; 26], such an approach does not pose any restriction on the estimates of NN weights.* ♢

INNARC Design

Throughout the process of controller design, f_2 and b_2 are approximated by the outputs of the corresponding neural networks and the tuning laws for NN weights are given in (14).

Considering the error indices $z_1 = x_1 - x_{1d}$ and $z_2 = \dot{z}_1 + k_{1,s} z_1$ with $k_{1,s}$ being a positive constant, the objective of controller design is to make both z_1 and z_2 as small as possible. Based on the basic idea of ARC [21], the following controller law is proposed

$$u = \underbrace{\frac{1}{\hat{b}_2}\left[-\hat{f}_2 - k_{1,s}\dot{z}_1 + \ddot{x}_{1d} - z_1\right]}_{u_a} - \frac{k_{2,s1}}{b_{l,2}} z_2 + u_{s2} \tag{27}$$

where u_a is the model compensation part, and u_{s2} is an extra robust term satisfying following conditions

$$z_2 \{Res_2 + b_2 u_{s2}\} \leq \epsilon_{z,2} \tag{28}$$

$$z_2 u_{s2} \leq 0 \tag{29}$$

where

$$Res_2 = [f_2 - \hat{f}_2] + [b_2 - \hat{b}_2] u_a + \Delta_2 \tag{30}$$

and $\epsilon_{z,2}$ is a positive constant.

Theorem 2. *With the use of identifier (9), controller (27), and tuning laws (14), the following system performance can be achieved*

A. In general, all the signals in closed system are bounded. The bound of tracking error and estimation error can be indicated by the following inequality

$$V_{ze}(t) \leq V_{ze}(0) exp(-Kt) + \frac{1 - exp(-Kt)}{K} \epsilon_{ze} \tag{31}$$

where $V_{ze} = \frac{1}{2}\left(e_2^2 + z_1^2 + z_2^2\right)$, $K = 2min\{a_2, k_{1,s}, k_{2,s1}\}$, *and* $\epsilon_{ze} = \epsilon_{e,2} + \epsilon_{z,2}$.

B. If there is no disturbance, the optimal NNs can match all the nonlinearities exactly, i.e., $\Delta_2 = \delta_{f_2} = \delta_{b_2} = 0$, *ideal values of all the hidden-output weights are within fictitious bounds, and PE condition (16) is satisfied, then both identification error and tracking error converge to zero asymptotically.* ♢

Proof. A. Considering the identification error in (12) and the time derivative of V_{z2}, $\dot{V}_{ze}$ is given as follows

$$\begin{aligned}\dot{V}_{ze} &= e_2\dot{e}_2 - k_{1,s} z_1^2 - \frac{b_2}{b_{l,2}} k_{2,s1} z_2^2 + z_2\{b_2 u_{s2} + Res_2\} \\ &\leq -a_2 e_2^2 + \epsilon_{e,2} - k_{1,s} z_1^2 - k_{2,s1} z_2^2 + \epsilon_{z,2} \\ &\leq -KV_{ze} + \epsilon_{ez}\end{aligned} \tag{32}$$

B. Result *B* in Theorem 1 indicates that $\lim_{t\to\infty} e_2 = 0$, which means that identification errors converge to zero asymptotically. Furthermore, since PE condition is satisfied, all the estimates of weights converge to their ideal values asymptotically, $\lim_{t\to\infty} Res_j = 0$ can be obtained from equation (30) by keeping in mind that $\Delta_2 = \delta_{f_2} = \delta_{b_2} = 0$. Consequently, inequality (32) changes to $\dot{V}_{ze} \leq -KV_{ze}$ when $t \to \infty$. Hence, $\lim_{t\to\infty} V_{ze} = 0$, which means that e_2, z_1 and z_2 converge to zero asymptotically. □

Remark 5. *While A of Theorem 2 shows that all signals in closed-loop system are under control and both identification error and tracking error can exponentially decay to certain small region, B indicates the possible asymptotic convergences of both tracking error and identification error, which achieves the ideal performance that NNs are used for. It is noted that [12; 13; 14; 15] cannot achieve such a performance.* ♢

INNARC DESIGN WITH UNKNOWN INPUT-HIDDEN WEIGHTS

In this section, the assumption that input-hidden weights are known is relaxed, and a more general case will be considered.

Design and Stability Analysis of RNN Identifier

Same as before, the following RNN identifier is proposed

$$\begin{aligned}\dot{\hat{x}}_2 = &-a_2 e_2 + \hat{f}_2 + \hat{b}_2 u \\ &- \left[\hat{\boldsymbol{\beta}}_{f_2}^T \boldsymbol{Y}_{f_2} + \hat{\boldsymbol{\beta}}_{b_2}^T \boldsymbol{Y}_{b_2} |u|\right] sgn(e_2) + u_{iden,2}\end{aligned} \tag{33}$$

Subtracting the second equation in (2) from (33) results in the following identification error equation

$$\begin{aligned}\dot{e}_2 = &-a_2 e_2 + [f_2^* - f_2] + \left[\hat{f}_2 - f_2^*\right] + [b_2^* - b_2] u + \left[\hat{b}_2 - b_2^*\right] u \\ &- \left[\hat{\boldsymbol{\beta}}_{f_2}^T \boldsymbol{Y}_{f_2} + \hat{\boldsymbol{\beta}}_{b_2}^T \boldsymbol{Y}_{b_2} |u|\right] sgn(e_2) + u_{iden,2} - \Delta_2\end{aligned} \tag{34}$$

By applying equations (6) and (7), the above identification error dynamics can also be written in the following form

$$\begin{aligned}\dot{e}_2 = &-a_2 e_2 + [f_2^* - f_2] + [b_2^* - b_2] u \\ &+ \left[\tilde{\boldsymbol{w}}_{f_2}^T (\hat{\boldsymbol{g}}_{f_2} - \hat{\boldsymbol{g}}'_{f_2} \hat{\boldsymbol{V}}_{f_2} \bar{x}_{a_2}) + \hat{\boldsymbol{w}}_{f_2}^T \hat{\boldsymbol{g}}'_{f_2} \tilde{\boldsymbol{V}}_{f_2} \bar{x}_{a_2} - d_{f_2,NN}\right] \\ &+ \left[\tilde{\boldsymbol{w}}_{b_2}^T (\hat{\boldsymbol{g}}_{b_2} - \hat{\boldsymbol{g}}'_{b_2} \hat{\boldsymbol{V}}_{b_2} \bar{x}_{a_2}) + \hat{\boldsymbol{w}}_{b_2}^T \hat{\boldsymbol{g}}'_{b_2} \tilde{\boldsymbol{V}}_{b_2} \bar{x}_{a_2} - d_{b_2,NN}\right] u \\ &- \left[\hat{\boldsymbol{\beta}}_{f_2}^T \boldsymbol{Y}_{f_2} + \hat{\boldsymbol{\beta}}_{b_2}^T \boldsymbol{Y}_{b_2} |u|\right] sgn(e_2) + u_{iden,2} - \Delta_2\end{aligned} \tag{35}$$

Based on identification error equation (35), the following gradient type of tuning laws are proposed along with projection mapping [19]

$$\begin{aligned}
\dot{\hat{\boldsymbol{w}}}_{f_2} &= \mathbf{Proj}_{\hat{\boldsymbol{w}}_{f_2}}\left[-\Gamma_{w,f_2}e_2\left(\hat{\boldsymbol{g}}_{f_2}-\hat{\boldsymbol{g}}'_{f_2}\hat{\boldsymbol{V}}_{f_2}\bar{x}_{a_2}\right)\right]\\
\dot{\hat{\boldsymbol{V}}}_{f_2} &= \mathbf{Proj}_{\hat{\boldsymbol{V}}_{f_2}}\left[\left(-\Gamma_{v,f_2}e_2\bar{x}_{a_2}\hat{\boldsymbol{w}}_{f_2}^T\hat{\boldsymbol{g}}'_{f_2}\right)^T\right]\\
\dot{\hat{\boldsymbol{\beta}}}_{f_2} &= \mathbf{Proj}_{\hat{\boldsymbol{\beta}}_{f_2}}\left[\Gamma_{\beta,f_2}|e_2|\boldsymbol{Y}_{f_2}\right]\\
\dot{\hat{\boldsymbol{w}}}_{b_2} &= \mathbf{Proj}_{\hat{\boldsymbol{w}}_{b_2}}\left[-\Gamma_{w,b_2}e_2u(\hat{\boldsymbol{g}}_{b_2}-\hat{\boldsymbol{g}}'_{b_2}\hat{\boldsymbol{V}}_{b_2}\bar{x}_{a_2})\right]\\
\dot{\hat{\boldsymbol{V}}}_{b_2} &= \mathbf{Proj}_{\hat{\boldsymbol{V}}_{b_2}}\left[\left(-\Gamma_{v,b_2}e_2u\bar{x}_{a_2}\hat{\boldsymbol{w}}_{b_2}^T\hat{\boldsymbol{g}}'_{b_2}\right)^T\right]\\
\dot{\hat{\boldsymbol{\beta}}}_{b_2} &= \mathbf{Proj}_{\hat{\boldsymbol{\beta}}_{b_2}}\left[\Gamma_{\beta,b_2}|e_2u|\boldsymbol{Y}_{b_2}\right]
\end{aligned} \tag{36}$$

Theorem 3. *Using the identifier (33) along with tuning laws in (36), the following results hold*

A. In general, estimates of NN weights are bounded, and the square of identification errors e_2 exponentially converges to a region bounded in the following fashion

$$\lim_{t\to\infty} e_2^2(t) \le \frac{1}{a_2}\epsilon_{e,2} \tag{37}$$

B. If there is no disturbance and the optimal NNs can match all the nonlinearities exactly, i.e., $\Delta_2 = \delta_{f_2} = \delta_{b_2} = 0$, and all the states x_i and input u are bounded, then all identification errors go to zero asymptotically provided that true values of NN weights are within fictitious bounds.

C. If the discontinuous terms $sgn(\star)$ drop from identifier (33), the basic performance stated in A is still valid. ♢

Proof. **A.** It can be proven in the same way as that in Theorem 1.

B. Consider the following Lyapunov function

$$\begin{aligned}
V_{ea} = V_e + \frac{1}{2}\Big[&\tilde{\boldsymbol{w}}_{f_2}^T\Gamma_{w,f_2}^{-1}\tilde{\boldsymbol{w}}_{f_2} + \tilde{\boldsymbol{w}}_{b_2}^T\Gamma_{w,b_2}^{-1}\tilde{\boldsymbol{w}}_{b_2}\\
&+\mathrm{Trace}\{\tilde{\boldsymbol{V}}_{f_2}\Gamma_{v,f_2}^{-1}\tilde{\boldsymbol{V}}_{f_2}^T\} + \mathrm{Trace}\{\tilde{\boldsymbol{V}}_{b_2}\Gamma_{v,b_2}^{-1}\tilde{\boldsymbol{V}}_{b_2}^T\}\\
&+\tilde{\boldsymbol{\beta}}_{f_2}^T\Gamma_{\beta,f_2}^{-1}\tilde{\boldsymbol{\beta}}_{f_2} + \tilde{\boldsymbol{\beta}}_{b_2}^T\Gamma_{\beta,b_2}^{-1}\tilde{\boldsymbol{\beta}}_{b_2}\Big]
\end{aligned} \tag{38}$$

Following the assumptions $\delta_{f_2} = \delta_{b_2} = 0$, $f_2 = f_2^*$ and $b_2 = b_2^*$ hold. Furthermore, considering $\Delta_2 = 0$, from equation (35), $\dot{V}_{ea}$ satisfies $\dot{V}_{ea} \le -a_2e_2^2$. By Barbalat's lemma, it is known that $\lim_{t\to} e_2 = 0$.

C. It can be proven by the same way as that in the proof of **A**. □

Remark 6. *Due to the same reason stated in Remark 3, RNN identifier (33) approximates input-output relationship of the true plant very well.* ♢

INNARC Design

Theorem 4. *With the use of identifier (33), controller (27), and tuning law (36), the following system performance can be achieved*

A. In general, all the signals in closed system are bounded. The bound of tracking error and estimation error can be indicated by the following inequality

$$V_{ze}(t) \le V_{ze}(0)exp(-Kt) + \frac{1-exp(-Kt)}{K}\epsilon_{ze} \tag{39}$$

Proof. **A.** The result can be worked out by the similar manner as that in part A of the proof of Theorem 2. □

EXPERIMENTAL STUDIES

To investigate how well the proposed INNARC solves the control problem in reality, the proposed INNARC is applied to the control of linear motor drive system by neglecting its fast electrical dynamics (bandwidth above 1000Hz).

To simplify the implementation, it is chosen that $u_{iden,2} = -k_{iden,2}e_2$ with $k_{iden,2}$ being a positive constant. In order to experimentally investigate the approximation capability of RNN, unlike those done in [18; 19], the NN used to estimate f_2 does not assume any special structure. A common three-layer feedforward NN with hyperbolic tangent function as activation function, five hidden neurons and one bias neuron is used to estimate f_2. It means that $\hat{f}_2 = \sum_{i=1}^{5} w_{f_2,i}tanh(\hat{v}_{f_2,i}\bar{x}_{a_2}) + w_{bias}$. Subsequently, tuning laws for NN weights are given as $\dot{\hat{w}}_{f_2,i} = Proj_{\hat{w}_{f_2,i}}\left[-\gamma_{w_{f_2,i}}\left[tanh(\hat{v}_{f_2,i}\bar{x}_{a_2}) - \frac{1}{cosh^2(\hat{v}_{f_2,i}\bar{x}_{a_2})\hat{v}_{f_2,i}\bar{x}_{a_2}}\right]e_2\right]$, $\dot{\hat{v}}_{f_2,i} = Proj_{\hat{v}_{f_2,i}}\left[-\gamma_{v_{f_2}}x_2e_2\hat{w}_{f_2,i}\frac{1}{cosh^2(\hat{v}_{f_2}\bar{x}_{a_2})}\right]$, $\dot{\hat{w}}_{bias} = Proj_{\hat{w}_{bias}}\left[-\gamma_{w_{bias}}e_2\right]$, $\dot{\hat{w}}_{b_2} = Proj_{\hat{w}_{b_2}}\left[-\gamma_{w_{b_2}}e_2u\right]$, $\dot{\hat{\boldsymbol{\beta}}}_{f_2} = Proj_{\hat{\beta}_{f_2}}\left[\gamma_{\beta_{f_2}}sgn(e_2)\boldsymbol{Y}_{f_2}\right]$, where the fact that b_2 is a constant is used to simplify the NN for estimating b_2.

Parameters

The experiments are conducted on an epoxy core linear motor. The detailed experimental setup is given in [18]. The nominal normalized values of M and B are $M = 0.027$ and $B = 0.273$, respectively. In experiments, constant feedback gains are used to simplify the control law for real-time implementation. Specifically, $k_{1,s} = 400$, $u_{s2} = -\frac{k_{2,s2}}{b_{1,2}}z_2$,

and $k_{2,s1} + k_{2,s2} = 10$. $a_2 = 2000$ is used in RNN identifier. The parameters used for tuning laws are summarized in Table 1. Within the given bounds, the initial values of all NN weight estimates are simply set to be zero except that $\hat{w}_{b_2} = 20$ to avoid singularity.

Table 1. Parameters for Weight Estimates

estimates	$\hat{w}_{f_2,i}$	$\hat{v}_{f_2,i}$	$\hat{w}_{bias}$	$\hat{w}_{b_2}$	$\hat{\beta}_{f_2}$
lower bounds	-3	-3000	-3	10	0
upper bounds	3	3000	3	50	1
adaptation rates	40	1000	10^6	50	10^{-6}

Experimental Results

In experiments, the desired trajectory is a smooth point-to-point back-and-forth trajectory, which is described in Fig. 1. It can be seen that the maximal displacement of the desired trajectory is 0.1 m and the maximal speed is 0.02 m/s. For easy comparison, desired trajectory is chosen to be the same as that in [18].

In Fig. 2, it can be seen that the tracking error is within $\pm 5\mu m$ and mainly stays within $\pm 2\mu m$, which is in the same level as the measurement resolution level, i.e., $\pm 1\mu m$. As a matter of fact, the maximal magnitude of tracking error achieved by INNARC is $4.8\mu m$, which is smaller than the maximal magnitude of tracking error, $5.5\mu m$ achieved by DNNARC in [18]. The identification error e_2 is shown in Fig. 3, where the "actual" velocity is obtained by passing the backward differentiation of position signal through a low-pass filter with transfer function $\frac{100}{s+100}$. Since the resolution of position signal is $\pm 1\mu m$ and sampling time interval is 4×10^{-4} sec, the resolution of its differentiation is $\frac{\pm 1\mu m}{4\times 10^{-4}\ sec} = \pm 0.0025 m/s$. It is found that the error in Fig. 3 is within the "resolution" level.

To further investigate the performance of neural network estimating nonlinearity $F_n = Mf_2$, the "true" value of F_n needs to be found. From equation (2), it is found that $F_n = u - M\ddot{x}$ by assuming that disturbance $F_d = 0$. F_n can be calculated if M and $\ddot{x}$ is available. The nominal value $M = 0.027$ is known, and acceleration $\ddot{x}$ is approximated by passing the backward differentiation of the position signal through a filter $\frac{100s}{s+100}$. Then the "true" value of nonlinearity F_n is obtained and is shown in Fig. 4. The NN approximation of F_n is calculated by $\hat{F}_n = \frac{\hat{f}_2}{\hat{b}_2}$, and is shown in Fig. 5. It can be seen that the estimate of F_n can follow its "true" values very well except that it is a little bit noisy. It has been shown in [18] that NN approximation in DNNARC can only capture the features of the nonlinear force, it cannot approximate it very well. In this sense, NN approximation result in INNARC is better than that in DNNARC. It should also be noted that desired trajectories to be tracked in both cases are the same.

For completeness, the control input is shown in Fig. 6. Compared with the magnitude of nonlinear force shown in Fig. 4, it is found that, approximately half of the control effort is used to counteract the nonlinear force. It also means that, the control objective is achieved by intelligently using model information rather than by purely strong feedback as in robust control.

CONCLUSION

In this paper, an indirect neural network adaptive robust control (INNARC) scheme has been developed for the precision motion control of linear motor drive systems to achieve the dual objectives of having not only excellent output tracking performance but also good nonlinear forces estimation for secondary purposes such as prognostics and machine health monitoring. Departing from the usual direct NN control designs, the proposed INNARC completely separates the unknown nonlinearity estimation from the design of underline adaptive robust control law. By doing so, various practical limitations associated with the NN learning in direct designs are overcome as there is no more one-stone-two-birds problem. Specifically, the estimation via NNs in the proposed INNARC is actual system dynamics based with certain actual measured states as driving signals, as opposed to the tracking error dynamics based estimation process of the direct designs that is more prone to be corrupted by measurement noises due to the use of rather smaller magnitude of tracking errors as driving signals. Furthermore, various practical modification such as the explicit monitoring of persistent excitation conditions can be used to enhance the quality of the estimates. Theoretically, the proposed INNARC achieves a guaranteed robust performance for both the NN identifier and the closed-loop system; in general, when all the NN weights, including input-hidden layer weights and hidden-output layer weights, are tuned on-line, even in the presence of disturbances, both the prediction errors of the identifier and the output tracking errors of the overall system are shown to exponentially converge to small regions that can be tuned by designers. Furthermore, in the ideal case that unknown nonlinearities are in the approximation ranges of the corresponding neural networks and the input-hidden layer weights are known, the identification error asymptotically converges to zero in the absence of disturbances. Experimental results have been obtained to verify the effectiveness of the proposed INNARC in achieving excellent output tracking performance as well as good estimations of unknown nonlinear forces for other

secondary purposes.

REFERENCES

1. D. M. Alter and T. C. Tsao, "Control of linear motors for machine tool feed drives: design and implementation of h_∞ optimal feedback control," *ASME J. of Dynamic systems, Measurement, and Control*, vol. 118, pp. 649–656, 1996.
2. D. M. Alter and T. C. Tsao, "Dynamic stiffness enhancement of direct linear motor feed drives for machining," in *Proc. of American Control Conference*, pp. 3303–3307, 1994.
3. P. V. Braembussche, J. Swevers, H. V. Brussel, and P. Vanherck, "Accurate tracking control of linear synchronous motor machine tool axes," *Mechatronics*, vol. 6, no. 5, pp. 507–521, 1996.
4. P. R. Dahl, "Solid friction damping of mechanical vibration," *AIAA Journal*, vol. 14, no. 12, pp. 1675–1682, 1976.
5. B. Armstrong-Hélouvry, P. Dupont, and C. Canudas de Wit, "A survey of models, analysis tools and compensation methods for the control of machines with friction," *Automatica*, vol. 30, no. 7, pp. 1083–1138, 1994.
6. C. C. de Wit, H. Olsson, K. J. Astrom, and P. Lischinsky, "A new model for control of systems with friction," *IEEE Trans. on Automatic Control*, vol. 40, no. 3, pp. 419–425, 1995.
7. K.-I. Funahashi, "On the approximate realization of continuous mappings by neural networks," *Neural Networks*, vol. 2, pp. 183–192, 1989.
8. K. Hornik, "Approximation capabilities of multilayer feedforward networks," *Neural Networks*, vol. 4, pp. 251–257, 1991.
9. G. Cybenko, "Approximation by superpositions of sigmoidal function," *Mathematics of Control, Signals and Systems*, vol. 2, pp. 303–314, 1989.
10. T. Poggio and F. Girosi, "Networks for approximation and learning," *Proceedings of the IEEE*, vol. 78, no. 9, pp. 1481–1497, 1990.
11. J. Park and I. W. Sandberg, "Universal approximation using radial-basis-function networks," *Neural Computation*, vol. 3, pp. 246–257, 1991.
12. F. L. Lewis, A. Yesidirek, and K. Liu, "Neural net robot controller with guaranteed tracking performance," *IEEE Transcations on Neural Networks*, vol. 6, pp. 703–715, 1995.
13. M. M. Polycarpou, "Stable adptive neural control scheme for nonlinear systems," *IEEE Transcations on Automatic Control*, vol. 41, no. 3, pp. 447–451, 1996.
14. Y. Zhang, P. A. Ioannou, and C. C. Chien, "Parameter convergence of a new class of adaptive controllers," *IEEE Trans. on Automatic Control*, vol. 41, no. 10, pp. 1489–1493, 1996.
15. R. M. Sanner and J.-J. E. Slotine, "Gaussian networks for direct adaptive control," *IEEE Transcations on Neural Networks*, vol. 3, no. 6, pp. 837–863, 1992.
16. S. Chen and S. A. Billings, "Neural networks for nonlinear dynamics system modelling and identification," *International Journal of Control*, vol. 56, pp. 319–346, 1992.
17. J. Q. Gong and B. Yao, "Neural network-based adaptive robust control of a class of nonlinear systems in normal form," in *Proceedings of the American Control Conference*, (Chicago, Illinois, USA), pp. 1491–1423, June 28–30, 2000.
18. J. Q. Gong and B. Yao, "Neural network adaptive robust control with application to precision motion control of linear motors," *International Journal of Adaptive Control and Signal Processing*, vol. 15, no. 8, pp. 837–864, 2001.
19. J. Q. Gong and B. Yao, "Neural network adaptive robust control of nonlinear systems in semi-strict feedback form," *Automatica*, vol. 37, no. 8, pp. 1149–1160, 2001, Special Issue on Neural Networks for Feedback Control.
20. B. Yao and M. Tomizuka, "Smooth robust adaptive sliding mode control of robot manipulators with guaranteed transient performance," in *Proc. of American Control Conference*, pp. 1176–1180, 1994. The full paper appeared in *ASME Journal of Dynamic Systems, Measurement and Control*, Vol. 118, No.4, pp764-775, 1996.
21. B. Yao, "High performance adaptive robust control of nonlinear systems: a general framework and new schemes," in *Proc. of IEEE Conference on Decision and Control*, pp. 2489–2494, 1997.
22. B. Yao and M. Tomizuka, "Adaptive robust control of siso nonlinear systems in a semi-strict feedback form," *Automatica*, vol. 33, no. 5, pp. 893–900, 1997. (Part of the paper appeared in Proc. of 1995 American Control Conference, pp2500-2505).
23. L.-C. Fu, W.-D. Chang, J.-H. Yang, and T.-S. Kuo, "Adaptive robust bank-to-turn missile autopilot design using neural networks," *Journal of Guidance, Control, and Dynamics*, vol. 20, no. 2, pp. 346–354, 1997.
24. X.-B. Liang and T. Yamaguchi, "On the analysis of global and absolute stability of nonlinear continuous neural networks," *IEICE Transactions on Fundamentals of Electronics Communications and Computer Sciences*, vol. E80-A, no. 1, pp. 223–229, 1997.
25. M. Forti, S. Manetti, and M. Marini, "Necessary and sufficient condition for absolut stability of neural networks," *IEEE Transactions on Circuits and Systems–I: fundamental Theory and Applications*, vol. 41, no. 7, pp. 491–494, 1994.
26. K. Matsuoka, "Stability conditions for nonlinear continuous neural networks with asymmetric connection weights," *Neural Networks*, vol. 5, pp. 495–500, 1992.

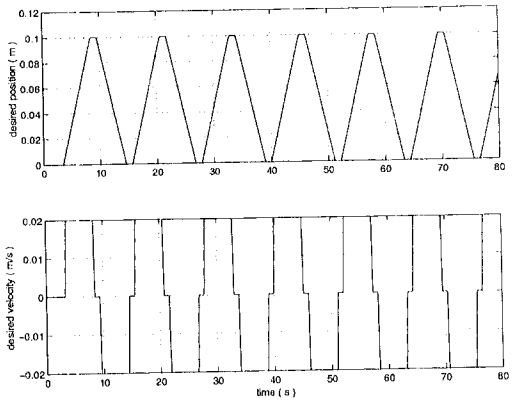

Figure 1. Position and velocity of the desired trajectory

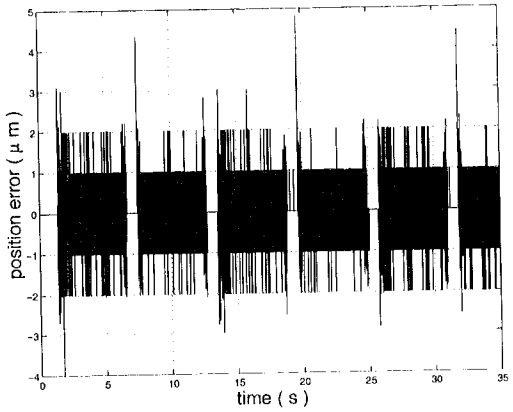

Figure 2. Time history of tracking error

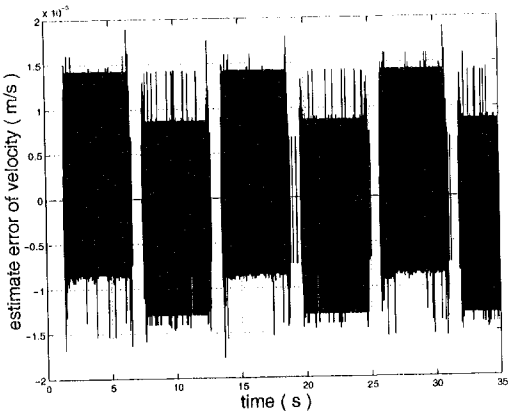

Figure 3. Estimate error of velocity

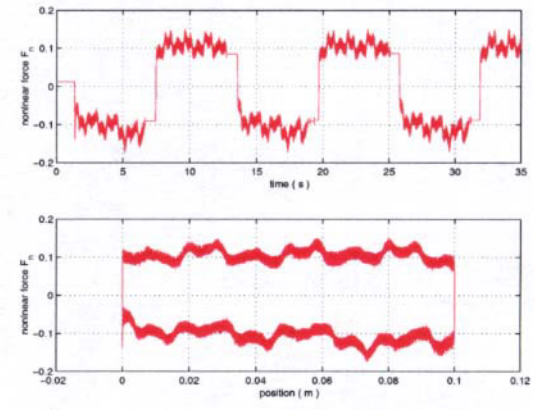

Figure 4. "True" value of normalized nonlinear force F_n

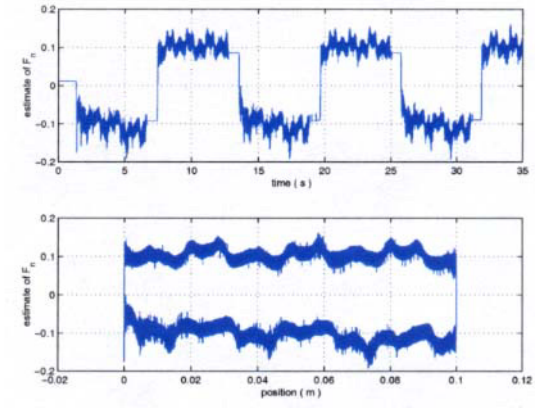

Figure 5. Estimated value of normalized nonlinear force F_n

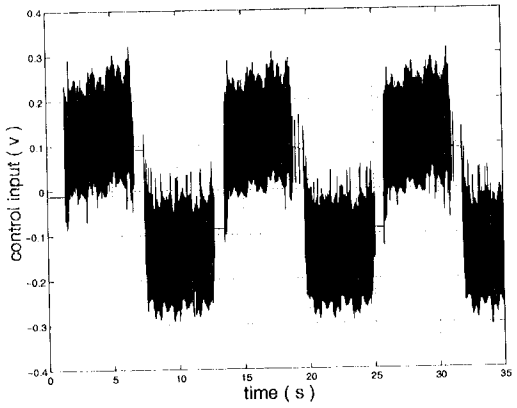

Figure 6. Control input